PHILOSOPHICAL TRANSACTIONS OF THE ROYAL SOCIETY A MATHEMATICAL, PHYSICAL & ENGINEERING SCIENCES

Microbial Mineralization of Organic Matter: Mechanisms of Self-Organization and Inferred Rates of Precipitation of Diagenetic Minerals [and Discussion]

M. L. Coleman, R. Raiswell, A. Brown, C. D. Curtis, A. C. Aplin, P. J. Ortoleva, M. Gruszczynski, T. Lyons, D. R. Lovley and G. Eglinton

Phil. Trans. R. Soc. Lond. A 1993 **344**, 69-87
doi: 10.1098/rsta.1993.0076

Microbial mineralization of organic matter: mechanisms of self-organization and inferred rates of precipitation of diagenetic minerals

By M. L. Coleman[1] and R. Raiswell[2]

[1] *Postgraduate Research Institute for Sedimentology, University of Reading, PO Box 227, Reading RG6 2AB, U.K., and BP Exploration, BP Research and Engineering Centre, Sunbury-on-Thames, Middx. TW16 7LN, U.K.*

[2] *Earth Sciences Department, University of Leeds, Leeds LS2 9JT, U.K.*

Carbonate concretions attract study because, unlike intergranular cements, they form conspicuous spheroidal or laterally extensive bodies. However, they pose a fundamental challenge to uniformitarianism because no concretions identical to geologically preserved ones are forming today. Nevertheless, understanding their origin can be accomplished by simulation of geological processes, using present-day processes and pore-water compositions. The successive reactions (mainly microbial) degrading organic-matter during sediment burial produce inorganic species which may form carbonate and sulphide minerals and can be characterized by stable isotope and chemical compositions. Pyrite-rimmed, spheroidal carbonate carbonate concretions (Jurassic) resulted from outward diffusion of microbially produced sulphide which reacted with inwardly diffusing iron. Extensive, bedded siderite concretions (Coal Measures) were formed by microbial reduction of Fe(III) which could only proceed because the reaction was buffered by precipitation of carbonate produced by methanogens degrading more deeply buried organic matter. By-products of the reactions may either inhibit or promote initiation of similar precipitation reactions locally. The former case leads to situations where initial random localization of reaction sites causes self-organized reaction within the sediment (applicable to the Jurassic example). Simulations of the Jurassic concretions' growth process, using present day pore-water solute concentrations of calcium, sulphide and iron, give results which correspond with the spatial distribution of mineral precipitates observed in geological samples. Calculated rates of mineral precipitation give minimum durations 7400 to 52000 years, much shorter than previous estimates. These results suggest that low rates of microbial sulphate reduction, relative to present day measured values, were needed and accord with the inferred depth of formation and pore-water sulphate concentrations.

1. Introduction: concretions and their significance

Diagenetic carbonate concretions occur in a variety of forms from perfectly defined spheroids to bedded, sheet-like bodies with diffuse-margins. This paper addresses the questions: What prevents development as uniform intergranular cements as commonly observed in sandstones? Why are some spheroidal and others bedded sheets? Attempting to answer these leads to a further question: How long do they take to form?

Phil. Trans. R. Soc. Lond. A (1993) **344**, 69–87
Printed in Great Britain

(a) *Distribution of intergranular diagenetic cements*

The particles which make up a clastic, sedimentary rock at deposition are not usually in chemical equilibrium with each other. Reactions with pore-waters, or with other solid components via pore-waters during burial, lessen chemical disequilibrium and may give various dissolution and precipitation reactions (chemical diagenesis). However, whereas location of dissolution reactions is controlled by reactivity of grains, controls on location of precipitation of mineral cements in intergranular pore-space are more complex. For example precipitation may be controlled by nucleation on specific mineral surfaces (e.g. diagenetic quartz usually nucleates on detrital quartz in sandstones) or may occur preferentially in the formerly more-permeable horizons which have focused the transport of solute-rich pore-water (Gluyas *et al.* 1993). Within an homogenous sandstone, cements are often distributed uniformly over volumes of a few cm^3, even if any two adjacent pores have different amounts of cement. However, occasionally, spheroidal, lenticular or sheet-like volumes of rock are extensively cemented with diagenetic carbonate (Thyne & Boles 1989; Gluyas & Coleman 1992). Stable isotopic analysis of these carbonate cements shows that some of the carbon was derived from organic matter (Irwin & Hurst 1983). Similar concretions occur in mudrocks, where carbonate cements may form most of the cemented volume. However, the existence and variety of forms of diagenetic concretions are more than academic curiosities.

(b) *Uses of concretions*

(i) *History of pore-water evolution*

The belief that concretions have grown sequentially from a nucleus led to work in which zoned variation in chemical and stable isotopic composition of carbonate was interpreted as a history of pore-water evolution (Irwin 1980; Coleman & Raiswell 1981; Gautier 1982; Curtis *et al.* 1986).

(ii) *Quantification of basinal mass flux*

Concretions have been used also in studies attempting to quantify changes in bulk sediment composition during burial diagenesis. The problem that constantly plagues such attempts is to determine the initial composition of the sediment, before any diagenetic processes occurred. Gluyas (1988) and Gluyas & Coleman (1992) proposed that samples of the original sediment were preserved within carbonate cemented sandstone concretions. Differences in composition of sediment within and outside concretions determine integrated mass flux in sedimentary basins during burial diagenesis. A similar approach was taken with mudrocks by Evans (1989), but Jordan *et al.* (1992) showed there were potential pitfalls in unrigorous data interpretations.

(iii) *Reservoir quality*

Sporadic occurrence of volumes of carbonate cement in a sandstone will affect its value as a petroleum reservoir. In the simplest case porosity will be occluded. However, and more importantly, bedded sheets of carbonate cement may have a beneficial or detrimental effect in either focusing or impeding flow, respectively, to producing wells. Unfortunately, concretionary horizons are encountered only as sections of relatively narrow diameter drill core. From such samples it is impossible to determine whether the concretion is a discrete spheroid or a continuous sheet.

PHILOSOPHICAL TRANSACTIONS OF THE ROYAL SOCIETY A MATHEMATICAL, PHYSICAL & ENGINEERING SCIENCES

(*c*) *Approach*

In this paper we discuss the biogeochemical processes by which carbonate concretions formed as a result of degradation of organic matter. We explore two contrasting cases: a Jurassic marine mudrock, bearing spheroidal calcite concretions with pyrite rims, and a Carboniferous non-marine mudrock with laterally extensive siderite cemented beds. We consider the relationships between the various processes, which then leads to formulation of their respective genetic models. For the first example we compute a quantitative model which is validated by calculations using present-day, measured values of pore-water chemistry. The model constrains rates of precipitation of diagenetic phases thereby allowing calculation of the duration of concretion growth.

2. Qualitative descriptions of processes

(*a*) *Relevant reactions and mass balance stoichiometries*

The presence of organic matter in sedimentary systems offers a significant energy source, because there are many potential oxidants of organic carbon in the pore-waters and mineral grains. Various microbial groups, adapted to perform specific reactions, exploit this energy source, often working in consortia with other groups. In this section we focus on the processes germane to concretions. The reactions are shown in schematic form to demonstrate the effect that they have on the inorganic components of the system, and particularly their ability to generate and precipitate carbonate. The key reactions are those which comprise the carbonate buffer. Dissolution or precipitation of carbonate is the principal pH buffer in this system because, in practice, pH values of pore-waters do not usually exceed the range 6.9–8.3 (Ben Yaakov 1973):

$$CO_2 + H_2O \leftrightarrow HCO_3^- + H^+, \tag{1}$$

$$Ca^{2+} + HCO_3^- \leftrightarrow CaCO_3^+ + H^+. \tag{2}$$

For uniformity of presentation, all carbonate species (which exist in mutual equilibrium; CO_2, HCO_3^-, CO_3^{2-}) will be shown as HCO_3^-, below. Many of the reactions involve generation or consumption of H^+ (hydrogen ions or acidity) but equally can be written in terms of consumption or generation of OH^- (hydroxyl ions or alkalinity), respectively. The convention adopted here expresses all reactions in terms of H^+ and additionally, for microbially mediated reactions, shows the mass balance requirements rather than details of biochemical pathways.

The equations above show that other reactions which consume H^+ are buffered by precipitation of carbonate (equations (1) and (2) driven to the right) while those generating H^+ will be buffered by carbonate dissolution.

Although aerobic oxidation of organic matter by dissolved oxygen is probably the most significant reaction in sedimentary systems, anaerobic processes are more relevant to this work and occur in organic-rich systems where aerobic processes deplete oxygen levels. Previous work on diagenetic carbonates resulting from organic matter degradation assumed sequential exhaustion of terminal electron acceptors (oxidants), producing vertical zonation of diagenetic processes and of the products (Irwin *et al.* 1977; Coleman & Raiswell 1981; Curtis *et al.* 1986). Coleman (1985) showed that the same sequence of products might be observed at any boundary

Table 1. *Diagenetic degradation of organic matter with geochemical and isotopic characteristics of diagenetic carbonates*

reaction	symbol	presence of Fe or Mn	$\delta^{13}C$	mineralogy
Mn(IV) reduction	MnR	yes	$-25‰$	rhodocrosite
Fe(III) reduction	FeR	yes	$-25‰$	siderite
sulphate reduction	SR	no	$-25‰$	calcite or dolomite
acetate methanogenesis	Me	yes	$+15‰$	calcite, dolomite or siderite
decarboxylation	D	no	$-25‰$	calcite, dolomite or siderite

between a reducing microenvironment and oxidizing surroundings. This zonal scheme, originally developed from analyses of pore-waters from steadily accumulated sediments (Claypool & Kaplan 1974; Froelich *et al.* 1979) is shown in the first two columns of table 1. Here we review previously published data, and suggest that the scheme does not apply perfectly to the diagenetic products of more episodically deposited sediments. Below we describe only those microbial processes relevant to the subsequent specific examples of concretion formation. The final process shown in table 1 is decarboxylation, which is the only definitively non-biological process, being the result of thermal degradation.

(*b*) *Stable isotope and chemical characterization of reactions*

Carbonates produced by the various reactions are also shown in table 1 and can be characterized by the application of three simple concepts (Curtis 1977; Irwin *et al.* 1977).

(*a*) Oxidized Mn and Fe enter the sedimentary system and until reduced, and available in solution, cannot be incorporated into diagenetically precipitated carbonate.

(*b*) Fe will react preferentially with sulphide, if available, and will not be incorporated into carbonates.

(*c*) Sedimentary organic carbon is depleted in ^{13}C ($\approx -25‰$, Schidlowski 1987) relative to seawater ($\delta^{13}C \approx 0‰$), and carbonate derived from degradation of organic matter inherits the carbon isotope composition of its precursor(s). The exception to this rule is methanic fermentation of acetate, where ^{13}C enriched carbonate is produced ($\delta^{13}C \approx +15‰$) to balance the extremely depleted methane formed at the same time.

Characteristics of carbonates produced by the various processes also are listed in table 1. Previous work (e.g. Coleman 1985) suggested that the characteristic diagenetic carbonates of MnR and FeR might have $\delta^{13}C \approx -5‰$ and $\delta^{13}C \approx -10‰$, respectively. This was explained as dilution of the organic isotopic signature with sea-water carbonate. Although probably valid for characterization of carbonates, it disguises the true nature of the microbial interactions which may occur. Consequently, the simple organic signature is shown (table 1).

(*c*) *Organic matter breakdown by fermentation*

Fermentation is one of the major processes which produces metabolites for subsequent microbial processes. Fermentation implies that the organic substrate is degraded, part becoming more oxidized, part more reduced, but in the absence of an

Table 2. *Mass balances for relevant diagenetic reactions*

reaction	mass balance	$HCO_3^-:H^+$
MnR	$4MnO_2+CH_3COOH+6H^+\rightarrow 4Mn^{2+}+2HCO_3^-+4H_2O$	2 : +6
MnR	$MnO_2+H_2+2H^+\rightarrow Mn^{2+}+2H_2O$	0 : +2
FeR	$4Fe_2O_3+CH_3COOH+14H^+\rightarrow 8Fe^{2+}+2HCO_3^-+8H_2O$	2 : +14
FeR	$Fe_2O_3+H_2+4H^+\rightarrow 2Fe^{2+}+3H_2O$	0 : +4
SR	$CH_3COOH+SO_4^{2-}\rightarrow HS^-+2HCO_3^-+H^+$	2 : −1
Me	$CH_3COOH+H_2O\rightarrow CH_4+HCO_3^-+H^+$	1 : −1
D	$R.CH_2COOH\rightarrow R.H+HCO_3^-+H^+$	1 : −1

external oxidant or reducer. Fermentation of carbohydrate gives acetate as one of the major products and its fate in other reactions is considered below. Molecular hydrogen, the other major product, is formed in about equal molar proportions. This process should not be confused with the methanic fermentation, discussed further below.

The relevant mass balance schemes are presented above in table 2, in the same order as in table 1. The most significant feature of each reaction, for the purposes of this work, is its ability to precipitate or dissolve carbonate. Equations (1) and (2) show that carbonate precipitation is governed by the ratio of HCO_3^- to the H^+ which is either generated or consumed by any reaction (table 2, last column). We use the convention that consumption of H^+, buffered by precipitation of carbonate, is shown as positive, while generation of H^+, which dissolves carbonate, is shown as negative.

Although there have been many references to microbial iron reduction in environmental systems (Sørensen 1982; Canfield 1989), it is only relatively recently that well-characterized, iron-reducing bacteria have been identified. Lovley (1991) isolated and cultured organisms that coupled oxidation of fermentation acids and/or hydrogen to Fe(III) reduction. Certain sulphate reducing bacteria reduce sedimentary Fe(III) directly, but only coupled to hydrogen oxidation (Coleman *et al.* 1993). Reaction mass balances involving both acetate and hydrogen as terminal electron acceptors are shown for FeR in table 2. The same respective organisms probably would also reduce Mn(IV) (Lovley 1993).

The reactions represented by FeR equations produce reduced Fe but also give the capability to precipitate carbonate, by consumption of H^+. All HCO_3^- produced (from acetate) could be precipitated but the overall reaction, which requires consumption of H^+ ions, would need to be buffered by precipitating carbonate produced by other reactions. This might allow then precipitation of more of the reduced Fe produced.

$$Fe^{2+}+HCO_3^-\rightarrow FeCO_3+H^+. \quad (3)$$

It may be that this necessity to promiscuously scavenge any available HCO_3^- persuaded Coleman (1985) to assign more positive values to MnR and FeR products and led to mis-assignment of siderite and ankerite as characteristic of methanogenesis in marine sediments (Gautier 1982; Curtis 1977). Siderite as the unequivocal product of FeR has now been described (Coleman *et al.* 1993).

The most significant and ubiquitous product of sulphate reduction is iron sulphide, usually precipitated initially as iron monosulphide, FeS, in Recent sediments but usually preserved as pyrite, FeS_2, in sedimentary rocks. Non-ferroan calcite with negative $\delta^{13}C$ associated with pyrite frequently has been ascribed to this process

PHILOSOPHICAL TRANSACTIONS OF THE ROYAL SOCIETY A MATHEMATICAL, PHYSICAL & ENGINEERING SCIENCES

(Irwin *et al.* 1977). The SR equation shows that although HCO_3^- concentration will be increased, the simultaneous production of H^+ will modify the carbonate buffer equilibria and determine whether carbonate is precipitated. Sulphate for the SR process is usually provided from sea water in which it is the second most abundant anion, after chloride. Therefore, in non-marine sediments sulphate commonly is absent and thus the principal anoxic process is methanogenesis, as exemplified in peat-marsh environments.

3. Qualitative genetic models for two examples

(a) *Concretions formed by SR: the Jet Rock*

There is overwhelming evidence that many carbonate concretions in the geological record owe their origin, either partly or wholly, to alkalinity generated by SR (Raiswell 1976; Hudson 1978; Coleman & Raiswell 1981). Such concretions are characterized by the following.

(i) Localized concentrations of pyrite. H_2S generated by SR at the concretion site is usually precipitated at (or near) the site as pyrite (but see later). After correcting for dilution by the carbonate, these concretions contain more pyrite than their surrounding sediments.

(ii) ^{34}S-depleted pyrite. During SR there is a kinetic isotopic fractionation effect (Goldhaber & Kaplan 1974) which gives H_2S depleted in ^{34}S compared to the original sulphate, typically about 45–50‰ lighter (Chambers & Trudinger 1979). For example, pyrite formed by SR from Jurassic seawater (*ca.* +17‰, Claypool *et al.* 1980) may be as light as −28 to −33‰. A trend towards heavier values because of closed system effects is seen frequently, but most systems retain some evidence of these characteristically light values.

(iii) ^{13}C depleted carbonate. The alkalinity generated by the decay of even low concentrations of organic matter is enough to overwhelm the alkalinity originally present in sea-water (for example decay of 1% organic C produces about 3×10^{-2} mol of alkalinity in a sediment of 85% porosity, compared to about 2×10^{-3} mol from sea water in the pores). Although $\delta^{13}C$ of SR carbonate is theoretically −25‰ (table 1), typical measured values are −12 to −18‰, suggesting mixing with another carbonate source, probably of marine origin.

Toarcian black shales of the Jet Rock (Port Mulgrave, Yorkshire, U.K.) enclose spheroidal concretions which are predominantly calcite. Pyrite occurs within the concretions but its concentration increases to the margins to form a sharply defined massive pyrite rim. Pyrite texture varies: the central part of the concretion contains framboidal pyrite while successive zones away from the centre show increasing amounts of euhedral pyrite overgrowths (Raiswell 1976). Geochemical compositions accord with the criteria for SR, above (Coleman & Raiswell 1981). The most recent attempt to describe their formation (Coleman & Raiswell 1993) involves arguments to explain the mineral zonation which depend on the balance between SR and FeR and whether an iron monosulphide precursor was involved in pyrite precipitation. An initial, pre-concretionary stage is postulated, in which precipitation of framboidal pyrite resulted from SR associated with Local FeR. The overall mass balance is given by

$$15CH_3COOH + 16SO_4^{2-} + 4Fe_2O_3 + 2H^+ \rightarrow 30HCO_3^- + 8FeS_2 + 16H_2O. \quad (4)$$

PHILOSOPHICAL TRANSACTIONS OF THE ROYAL SOCIETY A MATHEMATICAL, PHYSICAL & ENGINEERING SCIENCES

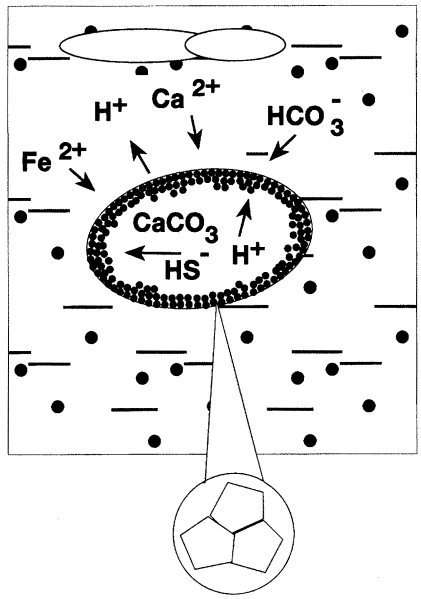

Figure 1. Conceptual model of growth for the Jet Rock concretions. SR without sufficient Fe^{2+} allowed precipitation of carbonate. Sulphide diffused out reacting with Fe^{2+}, precipitating euhedral pyrite and releasing H^+ which inhibited further, local carbonate precipitation. Additional carbonate was provided by dissolution of aragonitic fossils buffering their replacement by pyrite.

Although there was potential for some consumption of H^+, diffusive loss of the alkalinity generated to overlying seawater precluded carbonate precipitation. Subsequently, conditions for concretionary carbonate precipitation were created by direct precipitation of euhedral pyrite from pore-fluids with lower concentrations of reduced iron. During concretion growth the rate of generation of sulphide in the concretion core exceeded the rate of inward diffusion of reduced iron. SR in the absence of FeR can generate sufficient carbonate saturation to precipitate calcite (SR equation, table 2). Thus the resultant centrifugal diffusion of sulphide allowed precipitation of carbonate and defined the growth zone for euhedral pyrite, which formed the rim. (Similarly, later, pyrite casts of ammonites formed in the host mudrocks, the only sites where carbonate was available to be dissolved and buffer H^+ produced by SR.) The overall mass balance is given by equation (5).

$$7CH_3COOH + 8SO_4^{2-} + 4Fe^{2+} \rightarrow 4FeS_2 + 14HCO_3^- + 4H_2O + 6H^+. \quad (5)$$

However, separation of the site of sulphide generation from FeS_2 precipitation (associated with H^+ generation) gave rise to the mineral zonation. The concept of the process is shown in figure 1.

(*b*) *Concretions formed by other processes: Hepworth Coal Measure siderites*

Coal-measures sediments (Westphalian of Hepworth, Yorkshire, U.K.) contain various types of carbonate concretion; including extensive sheet-like siderite layers in non-marine mudrocks. Detailed geochemical analyses of the siderites (Curtis *et al.* 1986) showed symmetric vertical zonation about their central portions. The data were interpreted as recording the history of evolution of pore-water composition during burial of the sediment. Carbonate content, equivalent to contemporary porosity, defined the chronology of concretion growth during burial and compaction

Table 3. *Simulation of precipitation processes for diagenetic siderite*

relative proportion	process (as in table 2)	H^+	HCO_3^-	M^{2+}	$\delta^{13}C_{PDB}$(‰)
5	FeR(Ac)	70	10	40	−25
2	MnR(Ac)	12	4	8	−25
20	FeR(H_2)	80	0	40	−25
4	MnR(H_2)	32	0	8	−25
90	Me	−90	90	0	+15
	molar totals	104	104	96	average = +9.6

of sediment. Earliest-formed siderite with Mn/Fe ≈ 0.2 implies MnR as an important contributor to the pore-water system initially, which decreased relative to FeR during burial (Mn/Fe ≈ 0.02). However, carbon isotope compositions deny this interpretation: the Mn-rich siderites imply methanogenic carbonate ($\delta^{13}C > +10$‰) trending continuously to values indicating considerable contribution from decarboxylation reactions, for late-formed Mn-poor samples ($\delta^{13}C < -3$‰).

Reference to equations (MnR and FeR) show that both reactions consume H^+ and, therefore, must be buffered by precipitation of more carbonate than they produce. In contrast, methanogenesis and decarboxylation both produce equal molar amounts of HCO_3^- and H^+ (table 2). In extremely organic-rich sediments, such as these, there is sufficient residual organic matter after (below) FeR and MnR to allow both Me and D to occur. During burial of the sediment in which the concretion formed, the FeR and MnR processes possibly were buffered by upward diffusion of the products of Me and, increasingly, D with deeper burial.

It is possible to test this hypothesis by calculation of the expected chemical and isotopic compositions of analysed siderites. As an example of this approach we have attempted calculations to reproduce the composition of siderite described as early by Curtis *et al.* (1986). Assuming only equal proportions of acetate and hydrogen as substrates and ensuring buffering of H + generation and consumption (equation (2)), it is possible to simulate the observed compositions (table 3).

$\delta^{13}C$ at 9.6‰, is within the range for earliest siderites, 9.1–10.4‰. The only apparent discrepancy is the small deficit in metal ions available to be precipitated by the carbonate, about 8% molar of the total. The analysed samples show a similar discrepancy balanced by Ca and Mg, the combined abundance of which varies between 2 and 10%. This gives confidence that the simulation is viable, even if it is not a unique solution.

(*c*) *Comparative inferences*

The Jet Rock concretions are discrete nodular bodies and do not preserve a detailed history of pore-water evolution during their growth. Both features result from their mode of formation, which only allowed carbonate precipitation in the localized environment within the pyrite rim. In that case there was no *a priori* cause for sequential accumulation of calcite. Additionally, precipitation of carbonate produced extra H^+ which inhibited further carbonate precipitation beyond this zone. This can be considered a chemical negative feedback system which ensures that discrete nodular concretions formed.

In contrast, the driving force for precipitation of the Hepworth siderite was FeR and MnR within a system with abundant dissolved bicarbonate from other, deeper

reactions. Therefore, precipitation of siderite was limited only by the rate of FeR or MnR, and *sequential* accumulation of carbonate occurred within the concretionary bed. Neither Fe^{2+} nor Mn^{2+} diffused any appreciable distance beyond the site of reduction. FeR and MnR in that situation produced a positive chemical feedback causing extensive, rather than discrete, concretionary growth.

4. Quantitative growth model: applied to the Jet Rock concretions

(*a*) *Introduction to rate modelling*

In this section we attempt further to quantify the processes that operated in the geological past. We use as an example the calcite-pyrite concretions of the Jet Rock sequence, described above, in which the key reactions are FeR and SR. The basis of the approach is simulation of realistic processes which can be observed and measured in present, possibly comparable environments. There are major, and intractable, problems inherent in this approach. All the reactions involve precipitation from pore-waters. No ancient samples directly preserve pore-waters and there are no modern pore-water environments in which concretions of this type are seen to be forming.

There are two approaches to quantifiable validation of precipitation concepts. The more simple is to assess from modern pore-waters whether the total amounts of diagenetic material seen within sediments could be accumulated at a realistic rate. The second is to model in more detail the processes described qualitatively above and which might explain the concretions' size, shape and complex mineral zonation. After discussing precipitation processes, we describe both below.

(*b*) *Precipitation processes*

The involvement of SR in concretionary growth can be inferred not only from the diagenetic mineral assemblage but also from constraints from Recent pore-waters. It is supported by pore-water chemical studies of organic carbon-rich modern sediments, which almost invariably show the *potential* for $CaCO_3$ precipitation through high saturation indices (Berner *et al.* 1970; Sholkovitz 1973; Berner *et al.* 1978). Precipitation, however, seems to be extremely rare, possibly due to inhibition by adsorbed organic matter and/or phosphate on possible nucleation sites. The modern sediment data therefore pose a significant dilemma; all the characteristic SR signatures can be readily observed but there is generally little or no evidence of precipitation.

The lack of modern analogues for the geologically common occurrence of ancient carbonates attributed to SR has proved to be a major problem in attempting to estimate rates of concretionary growth. Theoretical models (Berner 1968) have been developed on the assumption that growth is diffusion limited,

$$t = R^2/2VD(C_\infty - C_R), \tag{6}$$

where R is the concretion radius (cm), V is the molar volume of the concretion cement ($cm^3\ mol^{-1}$), D is the diffusion coefficient ($cm^2\ s^{-1}$) and $(C_\infty - C_R)$ is the degree of supersaturation ($mol\ cm^{-3}$). In using these equations most workers on carbonate concretions have emphasized the difficulties in obtaining realistic estimates for the degree of supersaturation in ancient sediments (Boles *et al.* 1985). In fact, it seems certain that the assumption of diffusion-controlled growth is incorrect for the particular case of carbonate concretion growth in organic-carbon-bearing shales; instead growth is more likely to be surface-reaction controlled (Raiswell 1988).

PHILOSOPHICAL TRANSACTIONS OF THE ROYAL SOCIETY A MATHEMATICAL, PHYSICAL & ENGINEERING SCIENCES

Hence, even if realistic estimates of the degree of oversaturation could be made, then equation (6) could only provide minimum growth times.

(c) *Total quantity and rate of Jet Rock diagenetic calcite precipitation*

Canfield & Raiswell (1991*b*) have inferred rates of carbonate precipitation from the few modern sediments which show *indirect* evidence for carbonate precipitation. Three such sites have here been identified, although we emphasize that none of these show unequivocal evidence of recently formed, diagenetic carbonate. Their pore-water profiles show a systematic depletion in Ca^{2+} with depth; all pore-waters are oversaturated with respect to calcite and Ca^{2+} depletions range from 8 to 5.5 mM over the top metre of sediment at FOAM (Aller 1982), through 11 to 6 mM over the top 10–100 cm in Villefranche Bay (Gaillard *et al.* 1989) to a depletion of about 8 mM (evaporation corrected) over the top metre at Baffin Bay (Morse *et al.* 1992). These give mean Ca^{2+} gradients of 0.03, 0.04 and 0.07×10^{-6} mol cm^{-4} respectively.

If the density of concretion occurrence in a bed is s m^{-2}, ϕ the sediment porosity at the time of concretionary growth and all concretions are spherical, mean radius r, then the total volume of concretionary cement in 1 m^2 of sediment (which is equivalent to the thickness of a continuous cement bed) is $\frac{4}{3}\pi r^3 s\phi$.

For the Jet Rock case, 143 concretions occur in an area of 174 m^2 (Raiswell & White 1978), hence $s = 0.82$ m^{-2}. More than 75% of these concretions have a minor axis to major axis greater than 0.67 (Raiswell 1988) and sphericity is thus a fair approximation. The carbonate content of these concretions is about 85%, which is believed to approximately reflect the host sediment porosity at the time of growth (Raiswell 1976). The mean concretion radius is 0.185 m.

$$\text{The bed of equivalent thickness} = \tfrac{4}{3}\pi \times 0.185^3 \times 0.82 \times 0.85 = 0.018 \text{ m}.$$

So there is the same amount of concretionary carbonate in the Jet Rock concretions as there is in a laterally continuous pure limestone bed *ca.* 1.8 cm thick. This bed contains approximately 5×10^{-2} mol cm^{-2} $CaCO_3$ (assuming density of $CaCO_3$ is 2.65 g cm^{-3}).

Flux of Ca^{2+} to produce such a bed can be estimated using Ca^{2+} gradients (see above) and Ficks Law:

$$\text{flux} = -D \times (\text{rate of Ca depletion per unit depth}).$$

Using $D = 376$ cm^2 a^{-1} the modern sediment data give a flux of $-376 \times 0.03 \times 10^{-6}$ mol a^{-1} through 1 cm^2, or 9.4×10^{-6} mol a^{-1} at FOAM, and 15 or 26×10^{-6} mol a^{-1} at Villefranche and Baffin Bay. With these fluxes it would take about 1900–5300 years to form a bed equivalent thickness to the Jet Rock concentrations.

The slower estimates are more likely to be realistic. Both the Villefranche and Baffin Bay pore-water systems are unusual. The Villefranche sediments are penetrated at depth by karstic ground-waters (Gaillard *et al.* 1989) and the Baffin Bay system has elevated salinities due to high evaporation rates (Morse *et al.* 1992). Both these porewater systems are therefore perturbed in ways which could diminish the kinetic barriers to carbonate precipitation, and thus cause relatively rapid Ca^{2+} precipitation. The FOAM sediments are typical of near-shore organic-carbon-bearing sediments (about 1–2% organic carbon, generating up to 35 meq l^{-1} of alkalinity (Aller 1982)), but at least some of the Ca^{2+} depletion may be due to phosphate precipitation.

PHILOSOPHICAL TRANSACTIONS OF THE ROYAL SOCIETY A MATHEMATICAL, PHYSICAL & ENGINEERING SCIENCES

In contrast, siderite concretions have grown extremely rapidly, 15–20 cm diameter, in Recent salt-marsh sediments less than 60 years old (Pye *et al.* 1990). No explanation for the rate of growth was offered. However, two controls may be pertinent to this environment; siderite precipitation from pore-waters may not be inhibited, as is calcium carbonate, and tidal flushing of the sediment (K. Pye and P. Allison, personal communication 1992) could provide greatly enhanced transport of solutes.

(*e*) *Spatial zone model of Jet Rock concretionary growth*

Canfield & Raiswell (1991*a*) and Coleman & Raiswell (1993) have shown that the precipitation-driven diffusion models of Helfferich & Katchalsky (1970) can be used to show how the size, shape and position of the steady state diffusion-controlled zone of pyrite precipitation varies in the space between two reservoirs containing dissolved iron and dissolved sulphide. The model presented by Helfferich & Katchalsky (1970) is solved only for the one-dimensional case, i.e. for the linear variations along the axis between the two reservoirs. The results therefore only give a qualitative appreciation of the relative influences of the component variables, although even this limited approach has proved successful in explaining fossil soft part pyritization (Briggs *et al.* 1991; Raiswell 1992).

We use the Raiswell *et al.* (1993) modifications to Helfferich & Katchalsky's (1970) model to make it more realistic. These modifications provide a three-dimensional solution for the situation where a spherical body of organic matter decays by SR, generating H_2S which diffuses into a surrounding infinite reservoir of dissolved iron. The mathematical derivations are given in Raiswell *et al.* (1993), here we give the basis of the model and apply it to the pyrite-zoned Jet Rock concretions. Initially there will be a transient state of precipitation, since dissolved sulphide will diffuse away from the concretion site until the front of outward-diffusing sulphide (whose concentration decays with radial distance from the concretion) can all be precipitated by the dissolved iron as pyrite. The transient state then becomes a steady state, and pyrite formation will be maintained in a zonal configuration as long as the steady state exists. The model can only describe the steady state zonal configuration of pyrite precipitation but the transient state was probably of little quantitative significance because there are only low concentrations of the euhedral (concretionary) pyrite found in the concretion, apart from its margin. The model is idealized in a number of important respects, but does illustrate the types of pyritization which can result in a reaction-driven diffusion system, and it can explain the observed features of the concretionary system. The model also provides an estimate of the time to form the concretionary pyrite. This is probably the optimum which can be achieved in a rock system, as opposed to a modern sediment where pore water parameters can be measured directly:

$$j = \frac{2a^2(D_S C_S^0 + D_F C_F^0)^2 D_S D_F K}{r^4\{[D_F C_F^0 - (a/r)(D_S C_S^0 + D_F C_F^0)]^2 + 4 D_S D_F K\}^{\frac{3}{2}}}, \tag{7}$$

$$r_{j_{\max}} = \frac{a(D_S C_S^0 + D_F C_F^0)}{D_F C_F^0}, \tag{8}$$

where j is the rate of pyrite precipitation (mol cm^{-3} a^{-1}), D_F, D_S are the diffusion coefficients for dissolved iron and dissolved sulphide, respectively (cm^2 a^{-1}), C_F^0, C_S^0 are the constant reservoir concentrations of dissolved iron and dissolved sulphide

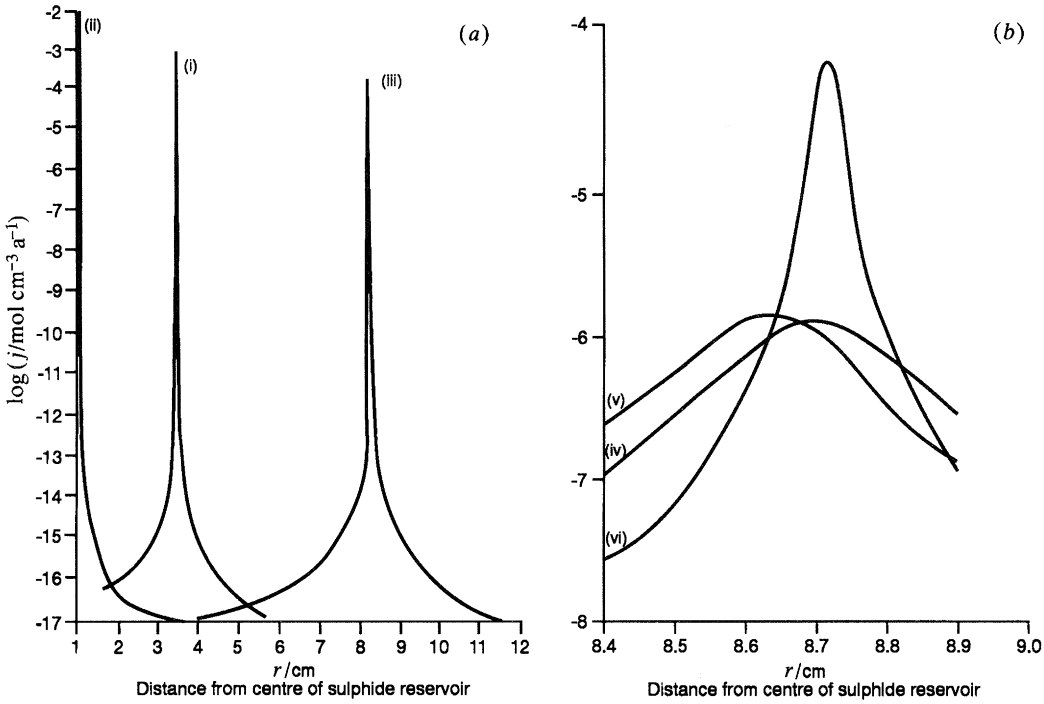

Figure 2. Modelled rate of pyrite precipitation as a function of distance from the sulphide reservoir. (*a*) (i) $C_S^0 = C_F^0 = 2.5 \times 10^{-9}$ mol cm^3; $C_S^0 C_F^0 = 6.2 \times 10^{-18}$. Substantial oversaturation with respect to pyrite, approaching saturation with FeS. (ii) $C_S^0 = 10^{-10}$, $C_F^0 = 2.5 \times 10^{-9}$ mol cm^{-3}, $C_S^0 C_F^0 = 2.5 \times 10^{-19}$. Substantial oversaturation with respect to pyrite, below FeS saturation. (iii) $C_S^0 = 7.5 \times 10^{-9}$, $C_F^0 = 2.5 \times 10^{-9}$ mol cm^3, $C_S^0 C_F^0 = 1.9 \times 10^{-17}$. Substantial oversaturation with pyrite, approaching FeS saturation. (*b*) All profiles have K increased to 1.66×10^{-20} mol cm^{-3}; (iv) $C_S^0 = 7.25 \times 10^{-8}$, $C_F^0 = 2.4 \times 10^{-8}$; (v) $C_S^0 = 1.12 \times 10^{-8}$, $C_F^0 = 2.4 \times 10^{-8}$; (vi) $C_S^0 = 7.25 \times 10^{-8}$, $C_F^0 = 1.55 \times 10^{-7}$.

(mol cm^{-3}), K is the solubility product for pyrite, expressed with respect to the reservoir species, a is the radius of spherical bacterial mass at the concretionary site (cm), r is any distance such that $a < r < \infty$ (cm).

These equations allow the rate of precipitation to be calculated, for a steady state, at any point between the two reservoirs. Values of D_S and D_F are taken for seawater from Boudreau & Canfield (1988) as 376 and 149 cm^{-2} a^{-1} respectively. In the model calculations a typical pore-water pH of 7.5 is assumed, given $K = 1.66 \times 10^{-28}$ in mol cm^{-3} (Raiswell *et al.* 1993), and the concentrations of dissolved sulphide and dissolved iron have been chosen by reference to pore-waters in analogous organic-rich modern sediments.

A variety of different, steady-state scenarios have been modelled and the results are shown in figure 2*a*. In effect the location of the zone of precipitation is controlled by the ratio of the reservoir fluxes. With $C_F^0 > C_S^0$ precipitation occurs at the site of the sulphide generating reservoir and, conversely with $C_S^0 > C_F^0$ the zone moves outward and may be located a considerable distance from the decay site. The position of each precipitation maximum (figure 2*a*) is quite sensitive to variations in the ratio of the reservoir concentrations, so that the mean radius of the zone of concretionary pyrite provides a unique value for C_S^0/C_F^0 (for any given value of a).

The thickness of the zone of precipitation, and the amount of pyrite precipitated,

Table 4. *Model results*

(*a*) Varying a; $R_{j_{max}} = 8.7$ cm; $j_{max} = 1.5 \times 10^{-4}$ mol cm^{-3} a^{-1} ($C^0_F = 2.5 \times 10^{-9}$ mol cm^{-3}, $K = 1.66 \times 10^{-28}$ mol cm^{-3}.)

	C^0_S
a/cm	mol cm^{-3}
1	7.65×10^{-9}
3	1.89×10^{-9}
5	7.38×10^{-10}
8	9.00×10^{-11}

(*b*) Constant a (1 cm) ($K = 1.66 \times 10^{-28}$ mol cm^{-3} $R_{j_{max}} = 8.7$ cm.)

C^0_S	C^0_F	$C^0_S \times C^0_F$	j_{max}
mol cm^{-3}	mol cm^{-3}	mol^2 cm^{-6}	mol cm^{-3} a^{-1}
7.6×10^{-9}	2.5×10^{-9}	1.9×10^{-17}	1.4×10^{-4}
2.3×10^{-8}	7.5×10^{-9}	1.7×10^{-16}	1.4×10^{-3}
6.9×10^{-8}	2.3×10^{-8}	1.5×10^{-15}	1.2×10^{-2}
2.4×10^{-7}	7.7×10^{-8}	1.8×10^{-14}	1.4×10^{-1}

also depend on the extent to which $C^0_S \times C^0_F$ exceeds $2K$. Where $C^0_S \times C^0_F$ only just exceeds $2K$, the precipitation zone is relatively thin, fairly symmetrical and will contain comparatively small amounts of pyrite (figure 2*a*). Conversely, where $C^0_S \times C^0_F \gg 2K$, the precipitation zone becomes wider and larger amounts of pyrite are also precipitated in this case. These three examples use fairly realistic values for C^0_S and C^0_F (7.5×10^{-9} to 10^{-10} mol cm^{-3}, equivalent to 0.1–7.5 μM of dissolved species in pore-water), in that modern pore-waters rarely exceed 100 μM for either dissolved sulphide or dissolved iron within the top few metres of sediment (Canfield & Raiswell 1991*a*). However, the analytical data for one of the concretions (sample UA, Raiswell 1976) allow some additional constraints to be placed on the model. Concretion UA has a thin pyritiferous zone at the margin, located 8.4–8.9 cm from the centre. Hence we can assume a model value for j_{max} at the mid-point, and equation (8) can be used to show that

$$C^0_S = (C^0_F/2.5)\,(8.65/a - 1). \tag{9}$$

Thus choosing a value for a determines the ratio, C^0_S/C^0_F, which in turn constrains the magnitude of j_{max}, as shown below.

Consider the effects of varying a. Holding C^0_F constant (at 2.5 μM) and varying a from 1 to 8 cm, determines C^0_S and fixes both the position (8.7 cm) and magnitude (1.5×10^{-4} mol cm^{-3} a^{-1}) of j_{max} (table 4*a*). Profiles of j across the zone of precipitation are also identical. Now, for any constant value of a (which fixes C^0_S/C^0_F) we can examine a range of C^0_S and C^0_F (< 100 μM, see above). In these circumstances j_{max} increases with increasing reservoir concentrations (table 4*b*) in direct proportion to the product $C^0_S \times C^0_F$.

It is notable that all these profiles have the very sharp maxima which are also seen in figure 2*a*. No combination of these variables can be found which provide a maximum at 8.7 cm and also give volumetrically significant amounts of pyrite at 8.4 and 8.9 cm. However, substantially less sharp maxima are produced for higher values of K (the solubility product). Thus figure 2*b* shows re-runs of the model with K increased from 1.66×10^{-28} to 1.66×10^{-20} mol cm^{-3}. These profiles give more realistic pyrite distributions.

5. Implications of qualitative and quantitative growth models

(a) Time for growth

The concretion itself further constrains the model system, when considered in the context of modern anoxic sediments. The concretionary pyrite post-dates a phase of diffuse pyrite formation throughout the sediment (Coleman & Raiswell 1981, 1993). Modern sediments at this stage of diagenesis typically have concentrations of dissolved Fe in pore-water which are relatively depleted (perhaps less than 100 μM; Canfield & Raiswell 1991*a*). C^0_F values approximately in this range produce the range of profiles of j with distance across the pyrite zone (figure 2*b*) which can be used to estimate the time for concretionary pyrite. This can be done by integrating the area under the curves to produce a mean value for j over the width of the pyrite zone. Profiles (iv), (v) and (vi) give mean rates of precipitation of *ca.* 7×10^{-7}, 7×10^{-7} and 5×10^{-6} mol cm^{-3} a^{-1}, respectively. Analytical data (Raiswell 1976) show that the zone contains 29.8% pyrite S, and thus has a density of *ca.* 4 g cm^{-3}. Thus the zone contains 3.7×10^{-2} mol cm^{-3} and the above rates indicate growth times of 52000 and 7400 years.

The model requirement by using increased K values (above saturation with pyrite) to produce wide zones of precipitation is geochemically reasonable. All the model systems are very over-saturated with respect to pyrite, in terms of *reservoir* concentrations. The existence of higher K in the zone of precipitation implies only that equilibrium is not reached. Substantial precipitation still occurs in order that the concentration product, $C^0_S \times C^0_F$, decreases to reach the specified K value. At these K values concentrations have decreased to levels at which the approach to equilibrium might be expected to be slow.

(b) Growth times from both methods compared

Growth estimates from the Ca^{2+} diffusion profiles (1900–5300 years) and the sulphide diffusion model (7400–52000 years) agree approximately, within an order of magnitude. Both are subject to uncertainty. However, Ca^{2+} depletion profiles are rare in modern anoxic sediments, because $CaCO_3$ precipitation is inhibited, but once inhibition is overcome through growth of fresh $CaCO_3$ surfaces, further precipitation may be rapid, at least initially. However, as these surfaces become contaminated, precipitation would cease until the kinetic barriers could again be overcome. This suggests that $CaCO_3$ precipitation may be sporadic, and that the Ca^{2+} profile estimates of time may be too low.

The major uncertainty in the sulphide diffusion model is the choice of realistic values for C^0_S and C^0_F. The C^0_S values in figure 2*b* could be sustained by typical rates of sulphate reduction observed in anoxic sediments; they do not require exceptionally easily metabolized organic matter and unusually high rates of sulphate reduction. Further work is in progress on this aspect of the models, but these growth estimates provide reasonable upper limits.

There is one further crucial observation to be made. The Jet Rock is believed to have accumulated at a rate of 30 cm of uncompacted sediment per 1000 years (P. Wignall, personal communication 1993). Only the shortest of the above growth times would allow concretionary growth to occur within the top few metres of sediment (which is typically the depth over which sulphate reduction occurs in modern anoxic sediments. The slower estimates would therefore imply that growth required a pause in deposition (see also Canfield & Raiswell 1991*b*, 1993). The implication that

PHILOSOPHICAL TRANSACTIONS OF THE ROYAL SOCIETY A MATHEMATICAL, PHYSICAL & ENGINEERING SCIENCES

concretionary horizons are the chemical expressions of physical sedimentological controls is a highly significant conclusion.

(*c*) *Nodular and bedded concretions*

The size and shape of the spheroidal concretions are controlled by the dynamics of diffusion from the centre of the concretion, and precipitation of the pyrite rim in a very tightly defined spatial zone. The sharp demarcation of the boundary of concretionary growth occurs only because the reaction which precipitates pyrite is one that does not produce a by-product which in turn enables further precipitation to occur. In fact, the reverse occurs, precipitation of pyrite also generates H^+ (equation (5)) and therefore inhibits local precipitation of pyrite or calcite. This is in marked contrast to the model presented for growth of the siderite concretionary horizons. In the latter case the impetus for carbonate precipitation is enhanced extent of reduction of Fe(III). If acetate is the substrate then some siderite will be precipitated directly. However, regardless of the electron donor, the by-product of the reaction is consumption of H^+ in excess of that required merely to precipitate any HCO_3^- produced. This effect causes further precipitation.

(*d*) *Positive and negative feedbacks*

Comparison of the two cases reveals that one of the key differences between the two processes is the nature of the by-products of the reactions and the effects that they have on subsequent reactions. For the pyritic and sideritic concretions they may be considered, respectively, as negative and positive feedback controls on the concretionary growth mechanism. The effect of a feedback mechanism can cause self-organization of the sedimentary system in which it operates.

(*e*) *Self-organization – spatial*

Coleman *et al.* (1979) suggested that rate of burial as well as organic matter content might be a primary control over selection of the bed in which diagenetic products might be concentrated. Rapid burial allows insufficient residence time in diffusive contact with oxygen or sulphate dissolved in overlying sea water leading to a preponderance of Me or D reaction products, rather than those from aerobic oxidation or SR. In the case of the Hepworth siderites the reason for enhanced FeR in the relevant beds is not clear. It might be either that there was an increased amount of reducible Fe(III) or that the conditions for FeR microbes to operate were especially suitable (e.g. nutrients, temperature, etc.). Regardless of the primary nucleation cause, the effect on the system as a whole was to concentrate in one bed the diagenetic carbonate produced from a much larger vertical section. Need for buffer capacity by precipitation of carbonate lowered its concentration locally and led to diffusion of more HCO_3^- to the site of precipitation from other beds.

Rate of burial seems a probable cause of enhanced SR in the Jet Rock system, where there is increased pyrite content relative to other beds (see above). However, lateral, rather than vertical concentration of diagenetic products is of greater interest here. The potential sites of nucleation for concretion growth were random and numerous initially. However, the radial diffusion and inhibitory effects of diagenetic by-products would soon have imposed a growth advantage on those nucleation sites which by chance developed sooner than their potential neighbours. If there had been a high enough density of diagenetic activity, then the result would have been establishment of a regular pattern of concretions; clearly the Jet Rock beds did not

PHILOSOPHICAL TRANSACTIONS OF THE ROYAL SOCIETY A MATHEMATICAL, PHYSICAL & ENGINEERING SCIENCES

behave in this way. Nevertheless, in this case, the resulting self-organization led to establishment of two main types of domain: the volume within the concretionary rims, where precipitation of diagenetic carbonate occurred, and the rest of the sediment, in which carbonate was dissolved (some of it being precipitated within the concretions).

6. Possibilities for further research and conclusions

(a) *Relationship of chemical and biological feedback*

In both the examples considered in detail above it is clear that normal chemical feedback mechanisms operate but microbiological generation of reactants is part of the process. What is not clear at present is the method by which the inorganic components interact with the specific microbial metabolic processes relevant here. There is a need to quantify the relationship between concentrations of stimulators or inhibitors and metabolic rates.

(b) *Amplification of climatically initiated sedimentary cyclicity*

Above we show that sideritic horizons resulted from concentration of the diagenetic products from a larger vertical section. Equally, Curtis & Douglas (1993) have commented on the relationship between the same horizons and climatic or sediment supply cyclicity. We speculatively identified higher concentrations of reducible Fe(III) or nutrients as the cause for intensive FeR. These two concepts are not incompatible. The next step will be to complete all the details in the path between climatic forcing and diagenetic self-organization and confirm whether microbial processes amplify the cyclic controls.

We thank Mandy Muggridge of BP for her help in drafting the figures.

References

Aller, R. C. 1982 Carbonate dissolution in near-surface terrigenous muds: role of physical and biological reworking. *J. Geol.* **90**, 79–95.

Ben Yaakov, S. 19973 pH buffering of pore water of recent anoxic marine sediment. *Limnol. Oceanogr.* **18**, 86–94.

Berner, R. A. 1968 Rate of concretion growth. *Geochim. cosmochim. Acta* **32**, 477–483.

Berner, R. A., Scott, M. R. & Thomlinson, C. 1970 Carbonate alkalinity in the pore waters of anoxic marine sediments. *Limnol. Oceanogr.* **15**, 544–549.

Berner, R. A., Westrich, J. T., Graber, R., Smith, J. & Martens, C. 1978 Inhibition of aragonite precipitation for supersaturated sea-water: a laboratory and field study. *Am. J. Sci.* **278**, 816–837.

Blatt, H. & Brown, V. M. 1974 Prophylactic separation of heavy minerals. *J. Sediment. Petrol.* **44**, 260–261.

Boles, J. R., Landis, C. A. & Dale, P. 1985 The Moeraki Boulders – anatomy of some septarian concretions. *J. Sediment. Petrol.* **55**, 398–406.

Boudreau, B. P. & Canfield, D. E. 1988 A provisional diagenetic model for pH in anoxic pore-waters. *J. mar. Res.* **46**, 429–455.

Briggs, D. E. G., Bottrell, S. H. & Raiswell, R. 1991 Pyritisation of soft-bodied fossils: Beechers Trilobite Bed, Upper Ordovician, New York State. *Geology* **19**, 1221–1224.

Canfield, D. E. 1989 Reactive iron in marine sediments. *Geochim. cosmochim. Acta* **53**, 619–632.

Canfield, D. E. & Raiswell, R. 1991*a* Pyrite formation and fossil preservation. In *Taphonomy: releasing the data locked in the fossil record* (ed. P. A. Allison & D. E. G. Briggs), ch. 7, pp. 337–387. New York: Plenum.

Canfield, D. E. & Raiswell, R. 1991*b* Carbonate precipitation and dissolutions: its relevance to fossil preservations. In *Taphonomy: releasing the data locked in the fossil record* (ed. P. A. Allison & D. E. G. Briggs), ch. 9, pp. 411–453, New York: Plenum.

Chambers, L. A. & Trudinger, P. A. 1979 Microbiological fractionation of stable sulphur isotopes. *Geomicrobiol. J.* **1**, 249–292.

Claypool, G. E., Holser, W. T., Kaplan, I. R., Sakai, H. & Zak, I. 1980 The age curves of sulfur and oxygen isotopes in marine sulfate and their mutual interpretation. *Chem. Geol.* **28**, 199–260.

Claypool, G. E. & Kaplan, I. R. 1974 The origin and distribution of methane in marine sediments. In *Natural gases in marine sediments* (ed. I. R. Kaplan), pp. 99–139. New York: Plenum Press.

Coleman, M. L. 1985 Geochemistry of diagenetic non-silicate minerals: kinetic considerations. *Phil. Trans. R. Soc. Lond.* A **315**, 39–56.

Coleman, M. L., Curtis, C. D. & Irwin, H. 1979 Burial rate a key to source and reservoir potential. *World Oil* **188**, 83–92.

Coleman, M. L., Hedrick, D. B., Lovley, D. R., White, D. C. & Pye, K. 1993 Reduction of Fe(III) in sediments by sulphate-reducing bacteria. *Nature, Lond.* **361**, 436–438.

Coleman, M. L. & Raiswell, R. 1981 Carbon, oxygen and sulphur isotope variations in carbonate concretions from the Upper Lias of N.E. England. *Geochim cosmochim Acta* **45**, 329–340.

Coleman, M. L. & Raiswell, R. 1993 Sources of carbonate and origin of zonation in pyritiferous carbonate concretions. *Am. J. Sci.* (In the press.)

Curtis, C. D. 1977 Sedimentary geochemistry: environments and processes dominated by involvement of an aqueous phase. *Phil. Trans. R. Soc. Lond.* A **286**, 353–372.

Curtis, C. D., Coleman, M. L. & Love, L. G. 1986 Pore water evolution during sediment burial from isotopic and mineral chemistry of calcite, dolomite and siderite concretions. *Geochim. cosmochim. Acta* **50**, 2321–2334.

Evans, I. J. 1989 Geochemical fluxes during shale diagenesis, an example from the Ordovician of Morocco. In *Water–rock interaction* (ed. D. L. Miles) pp. 219–222. Rotterdam: Balkema.

Froehlich, P. N., *et al.* 1979 Early oxidation of organic matter in pelagic sediments of the eastern equatorial Atlantic: suboxic diagenesis. *Geochim. cosmochim. Acta* **43**, 1075–1090.

Gaillard, J.-F., Pauwels, H. & Michard, M. 1989 Chemical diagenesis in coastal marine sediments: a study of the carbonate system. *Oceanogr. Acta* **12**, 175–187.

Gautier, D. L. 1982 Siderite concretions: indicators of early diagenesis in the Gammon Shale (Cretaceous). *J. Sediment. Petrol.* **52**, 859–871.

Gluyas, J. G. 1988 The quantification of sandstone diagenesis. BSRG 1988 (27th Annual Meeting of the British Sedimentological Research Group Abstracts). Cambridge, British Antarctic Survey.

Gluyas, J. G. & Coleman, M. L. 1992 Material flux and porosity changes during sediment diagenesis. *Nature, Lond.* **356**, 52–54.

Gluyas, J. G., Robinson, A. G., Emery, D., Grant, S. M. & Oxtoby, S. M. & N. H. 1993 The link between petroleum emplacement and sandstone cementation. In *4th Conf. on petroleum geology of NW Europe* (ed. J. R. Parker *et al.*). Geological Society of London.

Goldhaber, M. B. & Kaplan, I. R. 1974 The sulfur cycle. In *The sea* (ed. E. D. Goldberg), vol. **5**, pp. 569–655. New York: Wiley.

Helfferich, F. & Katchalsky, A. 1970 A simple model of interdiffusion with precipitation. *J. phys. Chem.* **74**, 231–240.

Irwin, H. 1980 Early diagenetic carbonate precipitation and pore fluid migration from the Kimmeridge Clay of Dorset. *Sedimentology* **27**, 577–591.

Irwin, H., Curtis, C. & Coleman, M. 1977 Isotopic evidence for source of diagenetic carbonates formed during burial of organic rich sediments. *Nature, Lond.* **269**, 209–213.

Irwin, H. & Hurst, A. R. 1983 Applications of geochemistry to sandstone reservoir studies. In *Petroleum geochemistry and exploration of Europe* (ed. J. Brooks), pp. 127–146. Oxford: Blackwell.

Jordan, M. M., Curtis, C. D., Aplin, A. C. & Coleman, M. L. 1992 Access of pore waters to carbonate precipitation sites during concretion growth. In *Proc. 7th Int. Symp. on Water–Rock Interactions* (ed. Y. Kharaka & A. S. Maest), pp. 1239–1242. Rotterdam: Balkema.

Lovley, D. R. 1991 Dissimilatory Fe(III) and Mn(IV) reduction. *Microbiol. Rev.* **55**, 259–287.

PHILOSOPHICAL TRANSACTIONS OF THE ROYAL SOCIETY A MATHEMATICAL, PHYSICAL & ENGINEERING SCIENCES

Morse, J. W., Cornwell, J. C., Arakaki, T., Saulwood, L. & Huerta-Diaz, M. 1992 Iron sulfide and carbonate mineral diagenesis in Baffin Bay, Texas. *J. Sediment. Petrol.* **62**, 671–680.

Pye, K., Dickson, J. A. D., Schiavon, N., Coleman, M. L. & Cox, M. 1990 Formation of siderite-Mg-calcite-iron sulphide concretions in intertidal marsh and sandflat sediments, north Norfolk, England. *Sedimentology* **37**, 325–343.

Raiswell, R. 1976 The microbiological formation of carbonate concretions in the Upper Lias of NE England. *Chem. Geol.* **18**, 227–244.

Raiswell, R. 1988 Evidence for the surface-reaction controlled growth of carbonate concretions in shales. *Sedimentology* **35**, 571–575.

Raiswell, R. 1992 The pyritisation of soft-bodied fossils. In *Proc. 7th Int. Symp. on Water–Rock Interactions* (ed. Y. K. Kharaka & A. S. Maest), pp. 301–304. Rotterdam: Balkema.

Raiswell, R., Whaler, K., Dean, S., Coleman, M. L. & Briggs, D. E. G. 1993 A simple three dimensional model of diffusion plus precipitation applied to localised pyrite formation in framboids, fossils and detrital iron minerals. *Marine Geol.* (In the press.)

Raiswell, R. & White, N. J. M. 1978 Spatial aspects of concretionary growth in the Upper Lias of NE England. *Sediment. Geol.* **20**, 291–300.

Schidlowski, M. 1987 Application of stable carbon isotopes to early biochemical evolution on earth. *A. Rev. Earth planet. Sci.* **15**, 47–72.

Sholkovitz, E. 1973 Interstitial water chemistry of the Santa Barbara sediments. *Geochim. cosmochim. Acta* **37**, 2043–2073.

Sørensen, J. 1982 Reduction of ferric iron in anaerobic, marine sediment and interaction with reduction of nitrate and sulfate. *Appl. Envir. Microbiol.* **43**, 319–324.

Thyne, G. D. & Boles, J. R. 1989 Isotopic evidence for origin of the Moeraki septarian concretions, New Zealand. *J. Sediment. Petrol.* **59**, 272–279.

Discussion

A. Brown. Fermentation produces hydrogen. Also, Fe may be precipitated as siderite, $FeCO_3$ rather than sulphides.

M. L. Coleman. See Coleman *et al.* (1993) for details of microbial iron reduction with H_2.

C. D. Curtis. How do the ankerite/ferroan dolomite concretions fit into the picture?

M. L. Coleman. There may be two causes: (*a*) nucleation on pre-existing primary carbonate; (*b*) wholly diagenetic carbonate. Possibly some Fe^{3+} is reduced and fixes HCO_3^- generated by methanogenesis and thermal decarboxylation elsewhere in the system (waiting to be fixed).

A. C. Aplin. The model for the formation of pyrite rims around carbonate concretions involves a reaction between dissolved Fe^{2+} and HS^-. Why does FeS_2 form under these conditions rather than FeS? It is also interesting that the model requires significant local variations in pore-water chemistry since sulphide and iron are diffusing to the precipitation zone from opposite directions. What conditions might give rise to such variations?

M. L. Coleman. FeS is precipitated from high Fe^{2+} and HS^- concentrations but at lower concentrations (low supersaturation for FeS) pyrite precipitates directly.

R. Raiswell. It is now possible to determine whether pyrite is primary or had a precursor phase.

P. J. Ortoleva. Are there examples with pyrite inside calcite? It is strange that it is always excluded.

M. L. Coleman. There is disseminated pyrite within the concretions. It is the precipitation of pyrite generating hydrogen ions which inhibits calcite beyond the sharp rim.

M. Gruszczynski. Why is silica not involved? H^+ is released which should mobilize SiO_2.

M. L. Coleman. I do not know. The controls on silica precipitation are poorly understood.

T. Lyons. Given the mechanisms and rates for concretion formation, it would be reasonable to expect at least incipient forms in modern sediments. Yet they are not common. Is this another failure of uniformitarianism? Should we look more carefully at modern sites with the requisite diagenetic conditions in association with prolonged breaks in sediment accumulation?

M. L. Coleman. The rate of change of sedimentation is important. Conditions probably include a pause in deposition, but with access to SO_4^{2-} which is then exhausted.

D. R. Lovley. One limiting factor is probably breakdown of organic matter.

G. Eglinton. There is a problem. Mineral formation must block the inward/outward movement of products and nutrients. This would limit activity, so do the bacteria control geometry to prevent this?

C. D. Curtis. Very recent work has shown that concretions do remain open to solute transfer, even in their centres.

A. Brown. In biofilms it is possible to see mineral precipitation around membranes/polymers less than one year old. They rapidly increase in thickness. Perhaps with enough biofilm/gel, a concretion would form.

D. R. Lovley. Mineral formation is generally extracellular and inorganic; microbes just reduce the Fe^{3+}.

M. L. Coleman. I can accept all these points! Microbial populations are agents of diagenetic change. We assume that microbes act at just the right rates; is this fair?

PHILOSOPHICAL TRANSACTIONS OF THE ROYAL SOCIETY A MATHEMATICAL, PHYSICAL & ENGINEERING SCIENCES